About Frequency Start of Motor-Compressor with Induction Motor for a Mainline Electric Locomotive

MIKHAIL PUSTOVETOV*[1], SVETLANA PUSTOVETOVA[2]
[1]Department of Electrical and Electronics Engineering
Don State Technical University
344000, Rostov region, Rostov-on-Don, Gagarin sq., 1
RUSSIA
[2]Rostov-on-Don College of Communications and Informatics
344082, Rostov region, Rostov-on-Don, Turgenevskaya st., 10/6
RUSSIA
*Corresponding author

Abstract: - The article examines the frequency start of an air compressor driven by a 3-phase induction motor. The frequency and voltage values are selected at which the motor's locked-rotor (startup) torque is close to the breakdown torque. Computer simulation of electromechanical processes is performed when induction motor powered by an autonomous voltage source inverter to estimate the inrush current.

Key-Words: - Induction motor, frequency start-up, auxiliary converter of electric locomotive, pulse-width control of voltage, load torque, locked-rotor torque, inrush current.

Received: May 23, 2024. Revised: January 28, 2025. Accepted: April 9, 2025. Published: July 31, 2025.

1 Introduction

The objective of this work is to check by calculation and by computer simulation the feasibility and identify the characteristics of the frequency start, as well as the factors influencing them, for the 3-phase 6-pole induction motor (IM) of type ANE200L6U2 with rated shaft power 22 kW, rated line voltage 380 V RMS and rated frequency 50 Hz, which driving air com-pressor onboard of a mainline electric locomotive with a starting load torque on the shaft $T_{load\_start} = 540$ N·m.

2 Problem Formulation

The load torque T_{load} at the beginning of the start is $2.5 \cdot T_{rated}$, with the start of rotation it drops to $0.28 \cdot T_{rated}$, reaching a value of $0.66 \cdot T_{rated}$ at 100 rpm, then the load torque increases slightly and reaches $T_{rated} = 214$ N·m at the rotation speed $n_{rated} = 980$ rpm, as shown in Fig. 1. Peak load torque is limited by overload safety clutch. On overload, the clutch disengages and separates input and output shafts as quickly as possible [1], [2], [3], [4]. This article does not take into account the dependence of the compressor load torque on the angle of rotation of the IM's rotor [5].

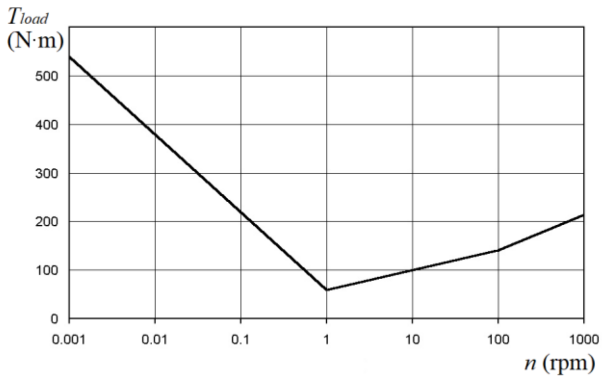

Fig. 1. Load torque on the motor-compressor shaft

To determine the most advantageous stator source frequency f_1 for IM starting, we will calculate at which f1 we will have a slip at breakdown torque $s_m = 1$ (we'd like to get a breakdown torque as locked-rotor (startup) torque). We will use the expression for s_m and the data in Table 1 for the rated mode, assuming that a value of the starting frequency of the supply voltage lies in the range of units of Hz [6, 7]:

$$s_m = \frac{c_1 r_2'}{\sqrt{r_1^2 + (X_{\sigma 1} + c_1 X_2')^2}}, \qquad (1)$$

where $c_1 \approx 1 + \dfrac{L_{\sigma 1}}{L_m}$.

Table 1. The parameters of T-shaped equivalent circuit (Steinmetz equivalent magnetic-electric circuit [8], [9]) for IM of type ANE200L6U2 at different modes

f_1 **(Hz)**	**50**	**33**	**25**	**16**	**50**
mode	**locked-rotor**				**rated**
$L_{\sigma 1}$ **(H)**	0.00124				
r_1 **(Ω)**	0.157				
L_m **(H)**	0.0523				
L_2' **(H)**	0.00161	0.00171	0.00177	0.00187	0.002235
r_2' **(Ω)**	0.266	0.249	0.238	0.221	0.159
In this work, iron losses are not taken into account					

$$c_1 \approx 1 + \frac{0.00124}{0.0523} = 1.0237 .$$

3 Problem Solution

Let us rewrite (1) for $s_m = 1$ through the inductances of the T-shaped equivalent circuit of IM:

$$1 = \frac{c_1 r_2'}{\sqrt{r_1^2 + (X_{\sigma 1} + c_1 X_2')^2}} = \frac{c_1 r_2'}{\sqrt{r_1^2 + (2\pi f_1)^2 (L_{\sigma 1} + c_1 L_2')^2}} .$$

At $f_1 = 1.94$ Hz and $s_m = 1$ the slip frequency will be $f_2 = s \cdot f_1 = 1.94$ Hz, which is comparable with the slip frequency at the rated mode: $f_2 = s \cdot f_1 = 0.02 \cdot 50 = 1$ Hz. At such frequencies the effect of current displacement in a squirrel cage conductors is practically not manifested, thus, to calculate the IM torque during frequency starting we have the right to use IM parameters for the rated mode (Table 1). The expression for the locked-rotor (startup) torque of IM:

$$T_{start} = \frac{3 \cdot p \cdot V_{phase1}^2 \cdot r_2'}{2 \cdot \pi \cdot f_1 \cdot \left[(r_1 + c_1 r_2')^2 + (X_{\sigma 1} + c_1 X_2')^2 \right]} . \quad (2)$$

Let us determine the line voltage at start-up according to the scalar open loop control with constant V / f_1 ratio for $T_{load} = \text{const}$:

$$\frac{V_{line}}{f_1} = \text{const} ; \; \frac{380}{50} = \frac{V_{line\_start}}{1.94} ; \; V_{line\_start} = 14.7 \, \text{V},$$

where is the phase voltage at start-up with the wye stator winding connection scheme $V_{phase\_start} = V_{line\_start} / \sqrt{3} = 14.7 / \sqrt{3} = 8.5$ V RMS. At this voltage value, the startup torque is $T_{start} \approx 83$ N·m in accordance with Eq. (2), which is clearly insufficient for setting in motion the ANE200L6U2 with $T_{load\_start} = 540$ N·m. Since IM startup torque is directly proportional to the applied to stator voltage squared, then using the proportion method we correct the value of the line supply voltage to the value required for a guaranteed (with a reserve of 10-20% for the shaft torque of IM) start (see Table 2).

To ensure starting with $T_{start} / T_{load\_start} = 1.2$ for the case of power supply with f_1 = 2 Hz, we determine V_{line_start} from the ratio:

$$\frac{V_{line\_start_1}}{f_{1_1}} = \frac{V_{line\_start_2}}{f_{1_2}} = \text{const} ,$$

then $V_{line\_start_2} = \frac{f_{1_2}}{f_{1_1}} \cdot V_{line\_start_1}$. I.e. at $f_1 = 2$ Hz we have $V_{line\_start} = \frac{2}{1.94} \cdot 41.1 = 42.4$ V RMS. It will be initial point for constant V / f_1 ratio with DC boost. Without correction, the voltage value $V_{line\_start} = 42.4$ V RMS would correspond to the frequency of the supply voltage $f_1 = \frac{42.4 \cdot 50}{380} = 5.6$ Hz.

Table 2. Calculated characteristics guaranteed to ensure the start-up of IM of type ANE200L6U2 at $T_{load\_start} = 540$ N·m and $f_1 = 1.94$ Hz

Characteristic	$T_{start} / T_{load\_start}$ **(p.u.)**	
	1.1	1.2
T_{start} **(N·m) in accordance with Eq. (2)**	594	648
V_{line_start} **(V RMS)**	39.4	41.1

Simulation using OrCAD [10], [11], [12] confirmed that with a sinusoidal supply voltage V_{line_start} adjusted for the starting torque, the IM of type ANE200L6U2 with a shaft load according to Fig. 1 is guaranteed to start (see Table 3). It should be noted that in all cases of simulating the start of the IM in this work, the frequency and voltage value did not change during the simulation process.

Table 3. Simulation results of starting ANE200L6U2 at sinusoidal supply voltage

f_1	V_{line_start}	J	$\hat{i}$	I_{start}	n_1	s
Hz	V RMS	kg·m²	A	A	rpm	p.u.
1.94	40	0.5	117.1	57.4	38.8	0.561
2	43		124.5	51.3	40	0.41
		5	125.3	51.4		0.409

The following designations are used in Table 3: J - moment of inertia of rotating masses, reduced to the motor shaft; $\hat{i}$ - peak (instantaneous) inrush current of the IM; I_{start} - RMS value of current of the IM phase in steady-state mode, achieved as a result of starting; s - slip in steady-state mode; n_1 - IM synchronous speed at the given f_1.

Since the motor-compressor is powered by an autonomous voltage source inverter (AVSI) [13], [14], [15] with pulse-width control of voltage (PWC) (a sort of PWM with carrying triangle signal and modulating meander signal) with the number of output voltage pulses (each of equal width) per period of the fundamental harmonic $\varepsilon = 24$, we will determine the duty cycles (D) required to obtain the values of the fundamental (first) harmonic $V_{1line\_start} = 40$ V RMS and $V_{1line\_start} = 43$ V RMS. The amplitude of the fundamental harmonic of the phase voltage at the AVSI output with a 180-degree transistor conductivity duration

$$V_{1m\_phase} = \frac{2 \cdot V_d}{\pi} \cdot D. \tag{3}$$

At the AVSI DC link voltage $V_d = 648$ V DC and $D = 1$ (six step voltage [15]): $V_{1m\_phase} = \frac{2 \cdot V_d}{\pi} = \frac{2 \cdot 648}{\pi} = 412.739$ V. Thus, $\frac{V_{1m\_phase\_start}}{D} = \frac{\sqrt{\frac{3}{2}} \cdot V_{1line\_start}}{D} = 412.739$,

$D = \frac{\sqrt{\frac{3}{2}} \cdot V_{1line\_start}}{412.739}$. For $V_{1line\_start} = 40$ V RMS and $V_{1line\_start} = 43$ V RMS the duty cycles, respectively, are $D = 0.0791$ and $D = 0.085$. The simulation results presented in Table 4 show that the pulsed nature of the supply voltage leads to a noticeable increase in the instantaneous values of the IM current and an increase in slip, which makes the starting conditions for the converter quite difficult.

Table 4. Simulation results of starting ANE200L6U2 at supply voltage PWC

f_1	V_{1line_start}	J	$\hat{i}$	I_{start}	I_{m_start}	s
Hz	V RMS	kg·m²	A	A	A	p.u.
2	40	5	242.6	61.3	211.4	0.691
	43		258.3	56.9	211.3	0.482

For the designations in Table 4, index 1 denotes belonging to the fundamental harmonic of the output voltage of AVSI. I_{m_start} - amplitude of the motor phase current in the mode established as a result of starting-up.

It should be noted that the J value has no effect on the IM inrush current, since its peak value occurs at a time when setting in motion has not yet occurred.

Let us check the possibility of IM starting at supply voltage frequencies of 16, 25, 33 and 50 Hz under the condition of $\frac{V_{line}}{f_1} = \frac{380}{50}$ (V RMS)/Hz. The values of the starting torque of the ANE200L6U2, calculated according to Eq. (2) taking into account the data of Table 1, are given in Table 5. Rated value of the motor current $I_{rated} = 47$ A RMS.

Values of T_{start} close to those shown in Table 5 were obtained by OrCAD simulating. These values do not provide a start of IM at $T_{load\_start} = 540$ N·m. It should be borne in mind that the applied IM mathematical model [5], as well as Eq. (2) and other traditionally applied calculation methods, including the models mentioned in [8], give underestimated (often significantly underestimated) values of the torque on the unstable branch of the speed-torque curve compared to the experiment (for example in accordance with experiments IM of type ANE200L6U2 provides a locked-rotor torque of at least 535 N·m at $f_1 = 50$ Hz). According to [15, 16], the torque increase is provided by the flow of currents in the rotor steel between the squirrel cage bars.

Table 5. Calculated starting torques and peak inrush current ratios for ANE200L6U2

f_1 **(Hz)**	16	25	33	50
T_{start} **(N·m)**	394	420	409	364
at sinusoidal supply voltage				
$\hat{i} / I_{rated}$ **(p.u.)**	4.7	6.1	7.1	8.7
when powered by an AVSI with a PWC voltage				
$\hat{i} / I_{rated}$ **(p.u.)**	5.6	6.8	7.5	8.6

An example of computer simulation of successful setting in motion of the motor-compressor at $f_1 = 16$ Hz is shown in Fig. 2 (voltage and current for stator phase A).

4 Conclusion

Simulation of the motor-compressor start-up showed the following. For a given value of the moment of inertia, the behavior of the drive (whether it will accelerate or not) is determined by the rate of decrease in the load torque on the shaft with an increase in the rotational speed, i.e. the value of the rotational speed at which the rated or minimum load torque is achieved. The air gap torque of the IM has the character of damped oscillations in the initial period after turning-on the voltage. The peaks of the air gap torque exceed the initial load torque. An oscillatory dependence of the rotational speed of the drive in time domain is observed. That is, even after setting in motion, the speed oscillations can either damp to zero - there will be no acceleration of the drive, or the speed will increase to a steady-state non-zero value - acceleration will occur. Theoretically, there is a boundary state when the rotational speed could have undamped oscillations around a small average value for an unlimited time. In practice (even during computer simulation), such a boundary state apparently cannot be achieved. Analysis of the average values of the air gap torque and the load torque during the simulation showed that even a very small difference in the average values is decisive for whether the drive will accelerate or not. Thus, for a J given value, there is a certain limiting value of the rotational speed at which the rated (or lower) value of the load torque is achieved. Otherwise, this can be interpreted as a limiting rate of decrease in the load torque during acceleration $\frac{dT_{load}}{dn}$. With the J decrease, the limiting $\frac{dT_{load}}{dn}$ decreases too.

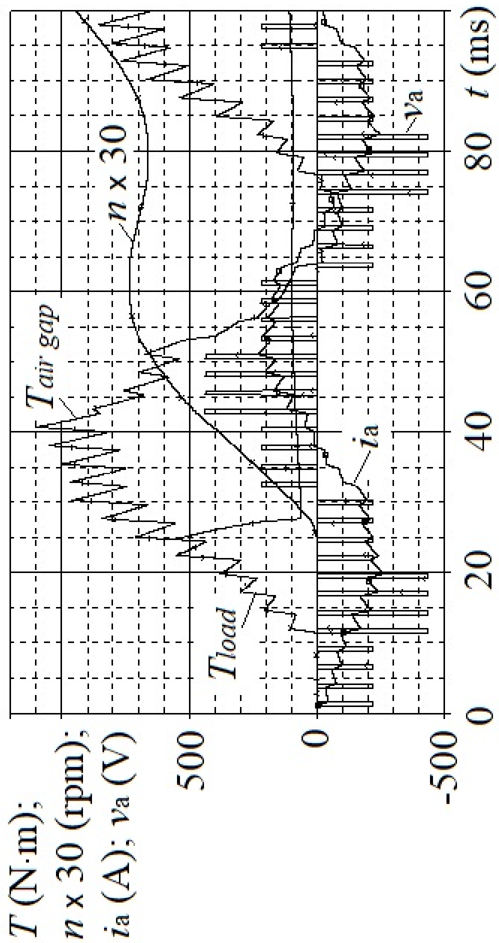

Fig. 2. Simulation results for successful setting in motion of the motor-compressor at $f_1 = 16$ Hz

Another task of the starting mode simulation was to determine the effect of the inverter output voltage generation method on the motor (inverter) phase inrush currents. The alternative methods considered were voltage PWC [17] with a carrier to modulating frequency ratio of $\varepsilon = 24$ and the amplitude method for voltage generation with a transistor conductivity duration of 180 electrical degrees (six step voltage). The starting option, in which the phase voltage remains unchanged with some decrease in frequency, is preferable from the point of view of the supply voltage value. For example, we had $f_1 = 48.4$ Hz and, accordingly, $V_{1m\_phase} = 253$ V. To start the motor-compressor, we will reduce the frequency to $f_1 = 45$ Hz. It should be noted that even without starting the motor-compressor, a decrease in frequency with an unchanged voltage value will cause an increase in the current of the already operating motor-fan and it's AVSI.

In the case of PWC we will determine duty cycles for the given values of V_{1m_phase} and V_d. We will determine the V_d value for the amplitude method for voltage generation for the given values of V_{1m_phase} at $D = 1$. The relationship between these three values is established for the selected control methods by Eq. (3). The calculation results for $J = 5$ kg·m^2 are summarized in Table 6. The initial phases of the voltages in all computational experiments remained the same. Thus, the value of the ratio $\hat{i} / I_{rated}$ for $f_1 = 45$ Hz in case of PWC reaches 7.6.

Table 6. Simulation results of starting-up a motor-compressor with a shaft load corresponding to Fig. 1

V_{1m_phase}	D	V_d	Did the start-up and subsequent acceleration take place?	The peak (instantaneous) inrush current of IM (A) (indices A and B indicate belonging to the corresponding phase of stator)
V	**p.u.**	**V DC**		
at $f_1 = 45$ Hz				
218.7	1.0	343.5	NO	-
253.0	1.0	397.4	YES	$\hat{i}_A = 348.3$
	0.613	648.0	YES	$\hat{i}_A = 357.9$
at $f_1 = 2$ Hz				
35.11	1.0	55.2	YES	$\hat{i}_A = 114.2$
	0.085	648.0	YES	$\hat{i}_B = 266.5$

It should be noted that if in Fig. 1 there is no load torque dip below rated value, then with the supply voltage parameters given in Table 6 at $f_1 = 45$ Hz acceleration becomes impossible. In this case, the inrush current does not change, since it corresponds to the very beginning of the start, when we have locked rotor condition.

The inrush current with the amplitude voltage regulation method is lower than with the selected PWC method. But at $f_1 = 45$ Hz the difference in current values is only 2.8%, which is insignificant (the inrush current value with amplitude voltage regulation is taken as the base value). And at $f_1 = 2$ Hz the difference is already 133.4%.

It should be recognized that from the point of view of the current value, starting with a large initial load torque is the most difficult operating mode of the motor-compressor. An additional increase in the instantaneous current values is due to the pulsed nature of the supply voltage. It should also be taken into account that, according to the data of [17], simulation gives some discrepancy with experiment in terms of instantaneous current values. Based on a comparison of the experimental and simulating data for the IM of type AZHV250M2RUHL2 which driving fan onboard of mainline electrical locomotive [5], [17], it can be recommended to multiply the current amplitude obtained as a simulation result by a factor equal to 1.3 - 1.35 in order to take into account the "greater mobility" of the experimental current. These factors should be taken into account when designing the auxiliary frequency converter for electric locomotives.

It is worth noting that induction motors with a double squirrel cage on the rotor, as well as with deep bars ones, are not recommended for operation with frequency converters [15], [18]. The fact is that the squirrel cage design of such electric motors is intended to achieve a high torque during direct starting [19], [20] from a source of unregulated voltage with a constant frequency due to the effect of current displacement in the conductors. During frequency starting, the final mechanical characteristic is formed from a set of characteristics obtained by changing the frequency and voltage. In this case, the effect of current displacement in the rotor conductors due to the virtually constant frequency of the current in the rotor for the fundamental harmonic will not manifest itself, but the non-sinusoidality of the voltage at the frequency converter output can, with such a squirrel cage design, lead to a clearly expressed displacement of higher harmonic currents into the upper part of the slot, which is fraught with overheating.

References:

[1] Overload Safety Couplings. [Online]. Available: https://zero-max.de/en/products/power-transmission-products/overload-safety-couplings/

[2] Safety Clutches. Overload Protection Using Torque Limitation. [Online]. Available: https://www.mayr-romania.ro/images/Mayr/download/cuplajelimitatoare/Ghid%20de%20selectare%20cuplaje%20limitatoare.pdf

[3] Ostyn F., Vanderborght B., Crevecoeur G., Overload Clutch With Integrated Torque Sensing and Decoupling Detection for Collision Tolerant Hybrid High-Speed Industrial Cobots, *IEEE Robotics and Automation Letters*, Vol. 7, No. 4, 2022, pp. 12601-12607. https://doi.org/10.1109/LRA.2022.3220527

[4] Lokesh V. Pithe, Avinash M. Badadhe, Automatic Electromechanical Single Plate Clutch with Overload Protection Roller Clutch for Machine Safety, *International Journal of Engineering Sciences*, Vol. 14, Iss. 1, 2021, pp. 26-33. https://doi.org/10.36224/ijes.140104

[5] Pustovetov M., Shukhmin K., Goolak S., Matijošius J., Kravchenko K., *Induction Motor Computer Models in Three-Phase Stator Reference Frames: A Technical Handbook*, Bentham Science Publishers Pte. Ltd. Singapore, 2023. https://doi.org/10.2174/97898151243091230101

[6] Voldek A.I., Popov V.V., *Electrical machines. Alternating current machines: Textbook for higher education institutions*, Moscow, Russia: Piter, 2010.

[7] Ion Boldea, Syed A. Nasar, *The induction machine hand-book*, CRC Press, 2002.

[8] Vučković V, Interpretation of a Discovery, *Serbian Journal of Electrical Engineering*, Vol. 3, No. 2, 2006, pp. 177–202. [Online]. Available: https://doiserbia.nb.rs/img/doi/1451-4869/2006/1451-48690603202V.pdf

[9] Aly Saandy T., Rakotomalala M., Said Mze, Toro A. F., Jaomiary A., Analytical Determining Of The Steinmetz Equivalent Diagram Elements Of Single-Phase Transformer, *International Journal of Scientific & Technology Research*, Vol. 4, Iss. 12, 2015, pp. 382-389. [Online]. Available: https://www.ijstr.org/final-print/dec2015/Analytical-Determining-Of-The-Steinmetz-Equivalent-Diagram-Elements-Of-Single-phase-Transformer.pdf

[10] Bolotovskii Yu.I., Tanazly G.I., *OrCAD. Modelirovanie “Povarennaya kniga” (OrCAD. “Cookbook” for Simulation)*, Moscow, Russia: Solon-press, 2005.

[11] Can E., Sayan H. H., PID and Fuzzy Controlling Three Phase Asynchronous Machine by Low Level DC Source Three Phase Inverter, *Tehnički vjesnik - Technical Gazette*, Vol. 23, Iss. 3, 2016, pp. 753-760. https://doi.org/10.17559/TV-20150106105608

[12] Holmes D. G., Lipo T. A., "Introduction to Power Electronic Converters," in *Pulse Width Modulation for Power Converters: Principles and Practice*, IEEE, 2003, pp.1-56, https://doi.org/10.1109/9780470546284.ch1

[13] Keown J., *OrCAD PSpice and Circuit Analysis*, 4th edition, Prentice Hall, 2000.

[14] Rashid M.H., *SPICE for Power Electronics and Electric Power*, 3rd edition, Boca Raton, USA: CRC Press, 2012.

[15] Binder A., *Motor Development for Electrical Drive Systems*, Iss. SS 2017. Germany: Technische universitat Darmstadt. Institut für Elektrische Energiewandlung. 149 p. [Online]. Available: https://www.ew.tu-darmstadt.de/media/ew/rd/ew_vorlesungen/lv_md/Text_book.pdf

[16] Kopylov I.P., *Mathematical modeling of electrical machines: Textbook for higher education institutions in the specialty "Electromechanics"*, 2nd ed., revised and enlarged, Moscow, Russia: Higher School, 1994.

[17] Pustovetov M., Refined Computer Model of Auxiliary Induction Motor of Electric Locomotive Powered by Autonomous Voltage Inverter, *DS Journal of Modeling and Simulation*, Vol. 1, Iss. 1, 2023, pp. 9-24. https://doi.org/10.59232/MS-V1I1P102

[18] Hilda Luthfiyah, Okghi Adam Qowiy, Arga Iman Malakani, Dwi Handoko Arthanto, Fauzi Dwi Setiawan, Teddy Anugrah Ramanel, Gilang Mantara Putra, Syamsul Kamar, Asep Andi Suryandi, An optimized stator and rotor design of squirrel cage induction motor for EMU train, *Journal of Mechatronics, Electrical Power, and Vehicular Technology*, Vol. 14, 2023, pp. 35-46. https://doi.org/10.14203/j.mev.2023.v14.35-46

[19] Konuhova M, Modeling of Induction Motor Direct Starting with and without Considering Current Displacement in Slot, *Applied Sciences*, Vol. 14, 9230, 2024. https://doi.org/10.3390/app14209230

[20] Nardo M. D., Marfoli A., Degano M., Gerada C., Rotor Slot Design of Squirrel Cage Induction Motors With Improved Rated Efficiency and Starting Capability, *IEEE Transactions on Industry Applications*, Vol. 58, No. 3, 2022, pp. 3383-3393. https://doi.org/10.1109/TIA.2022.3147156